ADAM12-directed ectodomain shedding of E-cadherin potentiates trophoblast fusion

M Aghababaei[1,2,6], K Hogg[3,4,6], S Perdu[1], WP Robinson[1,5] and AG Beristain*[,1,2]

Trophoblasts, placental cells of epithelial lineage, undergo extensive differentiation to form the cellular components of the placenta. Trophoblast progenitor cell differentiation into the multinucleated syncytiotrophoblast is a key developmental process required for placental function, where defects in syncytiotrophoblast formation and turnover associate with placental pathologies and link to poor pregnancy outcomes. The cellular and molecular processes governing syncytiotrophoblast formation are poorly understood, but require the activation of pathways that direct cell fusion. The protease, A Disintegrin and Metalloproteinase 12 (ADAM12), controls cell fusion in myoblasts and is highly expressed in the placenta localizing to multiple trophoblast populations. However, the importance of ADAM12 in regulating trophoblast fusion is unknown. Here, we describe a function for ADAM12 in regulating trophoblast fusion. Using two distinct trophoblast models of cell fusion, we show that ADAM12 is dynamically upregulated and is under the transcriptional control of protein kinase A. siRNA-directed loss of ADAM12 impedes spontaneous fusion of primary cytotrophoblasts, whereas overexpression of the secreted variant, ADAM12S, potentiates cell fusion in the Bewo trophoblast cell line. Mechanistically, both ectopic and endogenous levels of ADAM12 were shown to control trophoblast fusion through E-cadherin ectodomain shedding and remodeling of intercellular boundaries. This study describes a novel role for ADAM12 in placental development, specifically highlighting its importance in controlling the differentiation of villous cytotrophoblasts into multinucleated cellular structures. Moreover, this work identifies E-cadherin as a novel ADAM12 substrate, and highlights the significance that cell adhesion molecule ectodomain shedding has in normal development.
Cell Death and Differentiation (2015) 22, 1970–1984; doi:10.1038/cdd.2015.44; published online 24 April 2015

In mammalian development, the placenta forms the mechanical and physiological link between maternal and fetal circulations. In rodents and higher order primates, including humans, this transfer is achieved through extensive uterine infiltration by fetal-derived cells of epithelial lineage called trophoblasts.[1] Trophoblast differentiation is essential for optimal placental function, where the underlying molecular processes regulating specific functions of distinct trophoblast populations are strictly controlled. Defects in trophoblast differentiation associate with impaired placental function and directly impact fetal and maternal health.[2]

Within the placenta, progenitor trophoblasts (also called villous cytotrophoblasts; vCTs) overlie a well-defined basal lamina forming an organized, mitotically active epithelial layer. vCT differentiation into an overlying multinucleated structure called the syncytiotrophoblast (synCT) is a key event in placental development.[3] The synCT, composed of millions of nuclei sharing one common cytoplasm, directs nutrient and gas exchange between maternal and fetal circulations, and serves as the primary endocrine component of the placenta.[4] Its formation, function and continued renewal depends upon vCT fusion with existing synCT, where cellular competence for fusion is initiated by activation of the cyclic adenosine monophosphate (cAMP)/protein kinase A (PKA) pathway.[5,6] PKA directs multiple pathways important in trophoblast fusion, including the expression of the transcription factor glial cell missing 1 (GCM1).[7,8] Coordination and propagation of the fusion signal is controlled via gap junctions,[9,10] cytoskeletal reorganization[11,12] and remodeling of intercellular adhesion complexes.[13,14] Intercellular adherens junctions, composed of members of the cadherin family of cell adhesion molecules, are dynamically regulated during trophoblast syncytialization.[13,14] Described as important morphoregulators,[15] cadherins impact processes like cell sorting and differentiation, and thus mechanisms affecting cadherin expression or function can influence cell fusion.

A Disintegrin And Metalloproteinases (ADAMs) are Zn^{2+}-dependent proteases that play diverse roles in physiological and pathological processes. Characterized structurally by an N-terminal signal sequence followed by a prodomain, a metalloproteinase domain, a disintegrin domain, a cysteine rich region, an EGF domain, a transmembrane domain and a cytoplasmic tail,[16] ADAMs affect multiple cellular processes.[17] Expressed predominantly as transmembrane proteins, ADAMs function as cell surface 'sheddases', regulating the bioavailability of membrane proteins, such as

[1]The Child & Family Research Institute, Vancouver, British Columbia, Canada; [2]Department of Obstetrics & Gynecology, The University of British Columbia, Vancouver, British Columbia, Canada; [3]Centre for Genetic Diseases, MIMR-PHI Institute of Medical Research, Melbourne, Victoria, Australia; [4]Monash University, Melbourne, Victoria, Australia and [5]Department of Medical Genetics, The University of British Columbia, Vancouver, British Columbia, Canada
*Corresponding author: AG Beristain, Department of Obstetrics & Gynecology, Child & Family Research Institute, The University of British Columbia, 950 West 28th Ave, Room 371, Vancouver, British Columbia V5Z 4H4, Canada. Tel: +1 604 875 3573; E-mail: aberista@mail.ubc.ca
[6]These authors contributed equally to this work.
Abbreviations: ADAM12, A disintegrin and metalloproteinase 12; cAMP, Cyclic adenosine monophosphate; EVT, Extravillous cytotrophoblast; PKA, Protein kinase A; qPCR, Real-time polymerase chain reaction; synCT, Syncytiocytotrophoblast; vCT, villous cytotrophoblast

growth factors and their receptors,[16] cytokines[18] and cell adhesion molecules.[19]

Recently, our work has focused on the importance of ADAM12 in controlling trophoblast invasion and placental column outgrowth.[20] ADAM12, expressed as two distinct catalytically active splice variants, a full-length membrane-bound isoform (ADAM12L) and a truncated secreted variant (ADAM12S), is highly expressed in the placenta and localizes to invasive extravillous cytotrophoblast (EVT) subsets[20,21] and to the synCT layer.[22] Though ADAM12's localization to the syncytium suggests that it may play a role in directing trophoblast differentiation into multinucleated structures, the importance of ADAM12 in synCT formation has not yet been tested. Functional studies in mice identify ADAM12 as a regulator in myogenesis via effects on cell fusion,[23,24] and consistent with this, ADAM12S has been shown to direct osteoclast fusion in bone;[25] however, the molecular mechanism(s) central to these ADAM12-directed processes are poorly understood. In this study, we examine the importance of ADAM12 in regulating trophoblast fusion.

Results

ADAM12 localizes to multiple trophoblast subsets within placental villi.
Previous work localized ADAM12 to EVT subsets within distal anchoring columns[20,21] and to the synCT.[22] To confirm these findings, we re-examined ADAM12 localization in early (5–7 weeks gestation) and late (10–12 weeks gestation) first trimester placentae by immunofluorescence microscopy; the trophoblast markers hepatocyte growth factor activator inhibitor-1 (HAI-1), HLA-G and KRT7, as well as the proliferation marker Ki67 helped identify distinct trophoblast populations.[26] ADAM12 localized strongly to HLA-G[+] EVT columns and apically in the synCT (Figure 1a). ADAM12 positivity was also noted in trophoblasts localized proximal to Ki67^{+} EVTs and stochastically to HAI-1^{+} vCTs; ADAM12 preferentially localized to proliferative areas within floating villi noted by strong Ki67 positivity in serial sections (Figure 1a). Fluorescence signal specificity was ensured by probing placental villi with an IgG1 control antibody (Supplementary Figure S1).

To examine the expression of individual ADAM12 splice variants *in vivo* (the antibody used above identifies both isoforms), we examined ADAM12L and ADAM12S expression in fluorescence-activated cell sorting (FACS)-purified vCTs, column EVTs and mesenchymal core cells from placental villi using CD49f and HLA-G as subtype-specific markers (Figure 1b).[27,28] FACS-purified cell purity was verified by qPCR analysis using the pan-trophoblast marker KRT7, the EVT marker HLA-G and the mesenchymal marker VIM; whole placental villi served as a positive control (Figure 1c). Consistent with strong immunolocalization of ADAM12 to EVT columns, both ADAM12L and ADAM12S isoforms were expressed at higher levels in HLA-G^{+}CD49f^{lo} EVTs than in HLA-G^{-}CD49f^{hi} vCTs (Figure 1d). ADAM12S mRNA transcripts were expressed at higher levels in column EVTs compared with VIM-positive HLA-G^{-}CD49f^{-} mesenchymal cells; however, ADAM12L levels did not significantly differ (Figure 1d). Although ADAM12L was detected in placental

mesenchyme and vCTs, ADAM12S expression was restricted to EVTs, with little expression detected in vCTs (Figure 1d). Together, these findings demonstrate that ADAM12L/S are differentially expressed among trophoblast subtypes within placental villi, and that progenitor vCTs express moderate levels of ADAM12L and low levels of truncated ADAM12S.

ADAM12 expression increases during trophoblast fusion.
ADAM12's localization to the synCT suggests that its expression may be regulated during vCT fusion. To examine the temporal expression of ADAM12 during this process, vCTs from term placenta were cultured; these cells spontaneously differentiate to form multinucleated cells that resemble the synCT.[29] Fluorescence imaging of differentiating vCTs showed *de novo* expression of ADAM12 at 72 h, coinciding with the formation of multinucleated aggregates (Figure 2a). At 24 h prior to cell fusion, the ADAM12 signal was undetectable (Figure 2a). To visualize cell–cell fusion, the adherens junction molecule, E-cadherin, was probed to identify alterations in intercellular boundaries (Figure 2a); at 24 h, cells retained E-cadherin borders while cells cultured for 72 h showed re-organization of E-cadherin, characterized by diffuse and diminished staining at pericellular boundaries. To assess vCT purity, immunofluorescence analysis of the lineage markers KRT7 (epithelial) and vimentin (mesenchymal) was performed; these stains revealed >90% purity (Supplementary Figure S2).

Gene expression analysis of ADAM12L and ADAM12S showed that both isoforms increased over 72 h, with ADAM12L levels increasing fourfold and ADAM12S levels increasing over 10-fold (Figure 2b). Immunoblotting identified a predominant 68 kDa product that likely corresponds to proteolytically processed mature ADAM12; this product peaked at 48 and 72 h of culture (Figure 2c). Biochemical verification of vCT differentiation into multi-nucleated synCT-like structures was assessed by qPCR and immunoblot analyses probing for E-cadherin (CDH1), placental alkaline phosphatase (PLAP) and ERVW1, a gene encoding for the fusogenic retroviral envelope protein Syncytin-1. As expected, E-cadherin levels were markedly downregulated over 72 h, while PLAP levels reciprocally increased (Figures 2c and d). ERVW1 mRNA levels transiently increased at 24 h and then subsided by 72 h (Figure 2d).

PKA controls ADAM12 expression.
The PKA pathway plays a central role in trophoblast fusion, directing the expression of crucial transcription factors (e.g. GCM1) and fusogenic genes (e.g. ERVW1).[6,7] To this end, trophoblast differentiation into syncytial-like structures can be reproduced *in vitro* using the Bewo choriocarcinoma cell line in the presence of PKA agonists. We therefore examined whether ADAM12 induction during vCT differentiation could be reproduced in cAMP-differentiated Bewo cells. Visualization of untreated cells by immunofluorescence revealed that E-cadherin intercellular boundaries are retained over 72 h, while the ADAM12 signal remained absent (Figure 3a). Seventy-two hours post cAMP treatment, profound re-organization and loss of E-cadherin boundaries are observed (Figure 3a). Importantly, cAMP treatment results in *de novo* ADAM12 expression (Figure 3a). qPCR and immunoblot
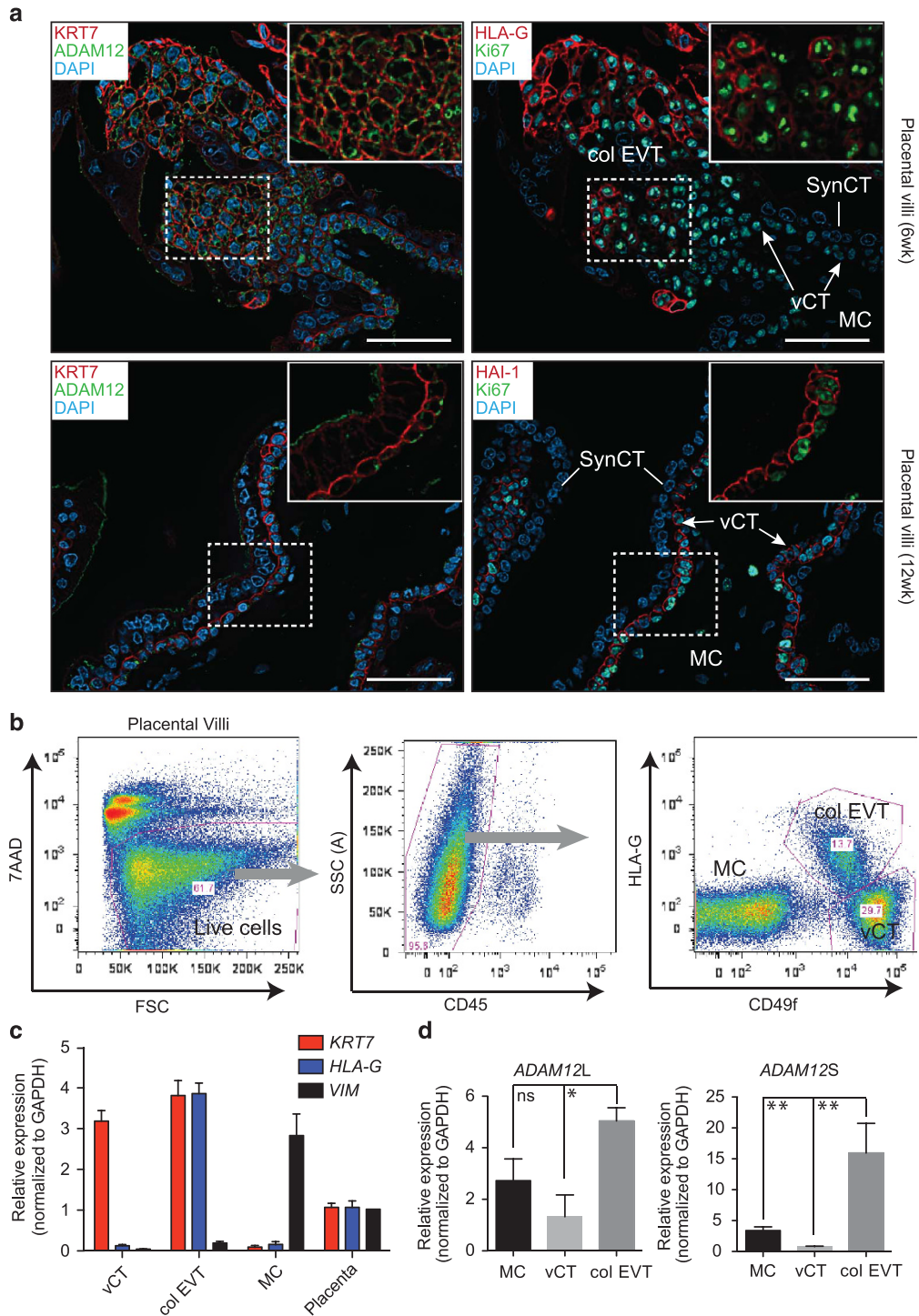
Figure 1 ADAM12 localizes to multiple trophoblast subtypes within placental villi. (**a**) Immunofluorescence images of first trimester placental villi (6 and 12 week gestation) immunostained with antibodies directed against ADAM12 (green) and the cytotrophoblast markers KRT7 (red), HAI-1 (red) and HLA-G (red); proliferative cells are labeled with an antibody targeting Ki67 (green) and DAPI-stained nuclei are labeled blue. Images are representative of placental villi from 5 to 7 weeks gestation ($N=5$) and 10 to 12 weeks gestation ($N=5$). Bar = 100 μm. 'col EVT' indicates EVT column; 'MC' indicates placenta mesenchymal core; 'synCT,' indicated by white lines, refers to the multinucleated synCT; 'vCT', indicated by white arrows, denotes vCTs. The perforated white box indicates enlarged inset image. (**b**) FACS plots demonstrate the trophoblast isolation strategy used to purify mesencymal core cells, columnar EVTs and vCTs. Live cells, depleted of CD31$^+$ (endothelial) and CD45$^+$ (immune) cells using immune-magnetic beads, were positively gated by 7AAD exclusion. Cells were further segregated by excluding CD45$^+$ immune cells and by cell surface labeling of HLA-G and CD49f. Cell subtype proportions are indicated within each gated population (percent of cells within FACS plot). (**c**) Trophoblast subtype purity was assessed by qPCR analysis targeting the pan-trophoblast marker *KRT7*, the EVT-marker *HLA-G* and the mesenchymal lineage marker *VIM*; placental villi (Placenta) served as positive control and relative gene expression reference. (**d**) qPCR analysis of *ADAM12*L and *ADAM12*S in FACS-purified mesenchymal core cells, vCTs and column EVTs. *GAPDH* was used for normalization. Results are presented as mean ± s.e.m. in bar graphs (*$P \leq$ 0.05, **$P \leq 0.01$) from four distinct placental villi specimens ($N=4$)
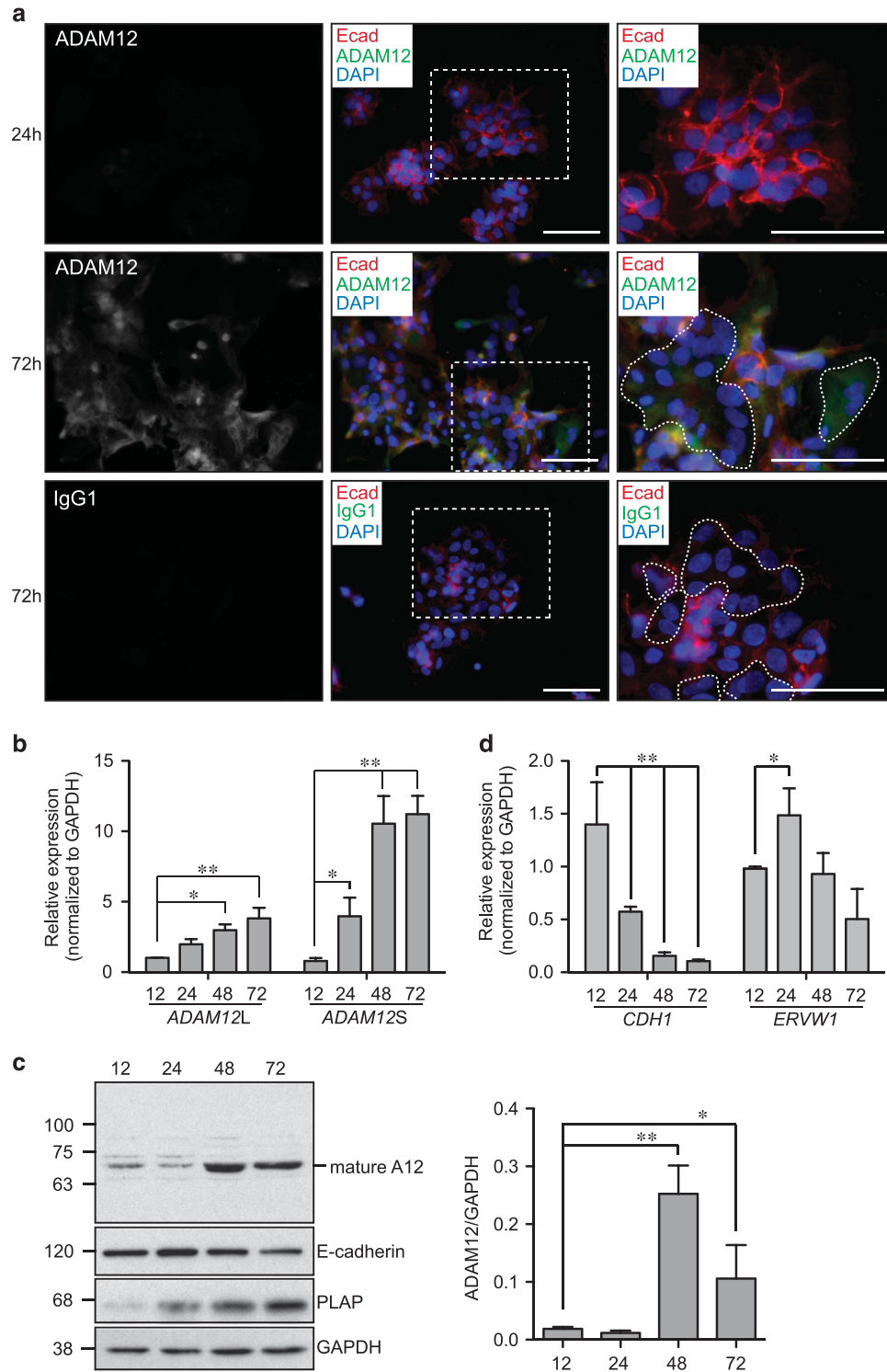
Figure 2 Spontaneous cytotrophoblast differentiation drives ADAM12 expression. (a) Representative immunofluorescence images of vCTs probed with antibodies directed against ADAM12 (green) and E-cadherin (Ecad; red) cultured for 24 or 72 h. DAPI-stained nuclei are labeled blue. Perforated white box shows magnified region while dotted line outlines multi-nucleated syncytial-like cell structures. Bar = 50 μm. IgG1-AlexaFluor-488 stain indicates the amount of secondary non-specific signal. (b) qPCR analysis of *ADAM12*L and *ADAM12*S in spontaneously differentiating vCTs over 72 h of culture. (c) Immunoblots showing ADAM12, E-cadherin and PLAP protein levels in whole cell lysates derived from primary vCTs cultured over 72 h. Molecular weights (kDa) are shown to the left and GAPDH indicates loading control. Mature ADAM12 (A12; 68 kDa) is highlighted and bar graph to the right denotes ADAM12 protein quantification over 72 h from four distinct cytotrophoblast cultures ($N = 4$) assayed by densitometry. (d) qPCR analysis of *CDH1* (E-cadherin) and *ERVW1* mRNA transcripts in vCTs cultured over 72 h. The results are presented as mean ± s.e.m. in bar graphs (*$P \leq 0.05$, **$P \leq 0.01$) from primary cytotrophoblasts isolated from four distinct term placentae ($N = 4$). All qPCR gene expression reactions were normalized to endogenous *GAPDH*

analyses confirmed that *ADAM12*L and *ADAM12*S transcripts and ADAM12 protein levels increase during Bewo differentiation, where the increase in *ADAM12*S is greater than *ADAM12*L (Figure 3b). The morphological changes in response to cAMP were characterized biochemically by

qPCR analysis and immunoblotting for E-cadherin (*CDH1*), *ERVW1* and PLAP. As expected, E-cadherin levels decreased during fusion, whereas PLAP and *ERVW1* (markers of differentiation and fusion) increased (Figures 3c and d). Interestingly, cAMP treatment in JEG3 trophoblastic
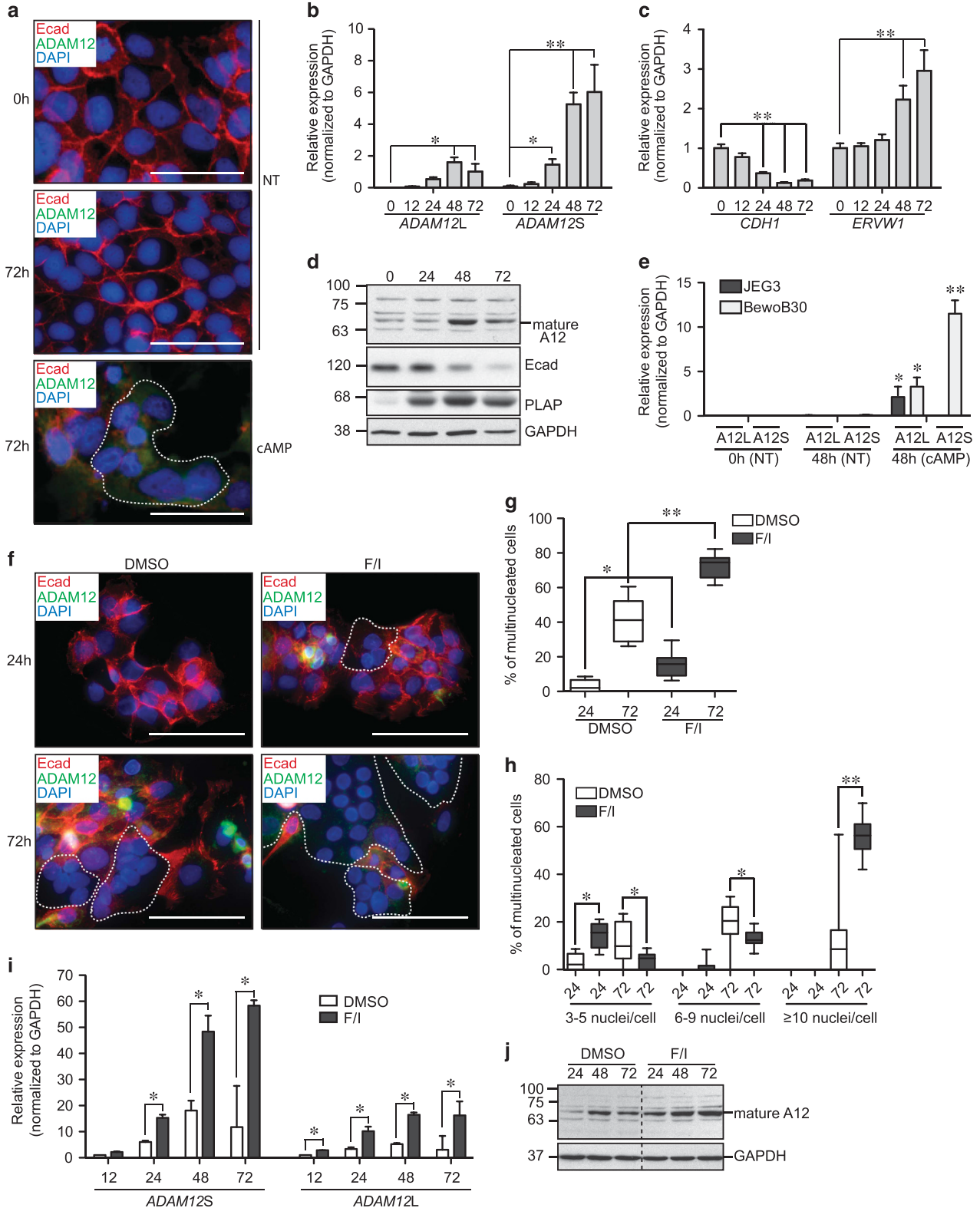
cells, which do not fuse in response to PKA stimulation, showed modest increases in *ADAM12*L and negligible increases in *ADAM12*S, suggesting that ADAM12S, and not ADAM12L, is the key isoform during fusion (Figure 3e).

To test whether PKA-accelerated syncytial formation in primary trophoblasts leads to increases in ADAM12 expression above the increases measured during spontaneous fusion, vCTs were treated with PKA agonists forskolin/IBMX (F/I) over 72 h. Treatment with F/I accelerated remodeling of E-cadherin at cell boundaries at 24 h, and by 72 h, multinucleated cells were abundant comprising > 70% of total cells (Figures 3f and g). Compared with spontaneously differentiating vCTs, F/I treatment increased the proportion of multinucleated cells at 24 h (F/I median = 15.75%, inter-quartile range (IQR) = 9.2–19.3; spontaneous median = 2.1%, IQR = 0.0–6.6) and 72 h (F/I = 74.5%, IQR = 65.8–77.2; spontaneous median = 41.2%, IQR = 28.9–52.2) (Figure 3g). The proportion of cells forming large multinucleated structures (≥ 10 nuclei) was also substantially greater in F/I-induced conditions (F/I median = 56.3%, IQR = 50.6–61.1; spontaneous median = 8.5%, IQR = 0.0–16.6) (Figure 3h). Importantly, F/I treatment increased *ADAM12*S and *ADAM12*L mRNA and ADAM12 protein levels, where the induction of *ADAM12*S was more pronounced than *ADAM12*L (Figures 3i and j).

To examine whether PKA directly regulates ADAM12 expression in trophoblasts, Bewo cells were transiently transfected with a luciferase ADAM12 promoter reporter construct. Following transfection, ADAM12 promoter activity was examined in cells untreated or treated with cAMP. Treatment with cAMP increased ADAM12 promoter activity (Figure 4a). Further, cAMP treatment increased *ADAM12*S and *ADAM12*L mRNA levels, as well as ADAM12 protein, and these cAMP-directed increases were blocked by the PKA inhibitor, PKI (Figures 4b and c). Together these findings demonstrate that PKA signaling drives ADAM12 expression during trophoblast fusion.

Loss of ADAM12 inhibits spontaneous trophoblast cell fusion. To interrogate ADAM12 in trophoblast fusion, primary vCTs were transfected with siRNAs (A12i5 and A12i8) targeting ADAM12. Cells treated with non-targeting scrambled siRNA (NS) or with transfection reagent alone served as controls. The efficacy of ADAM12-siRNA

knockdown in A12i5- and A12i8-transfected cells was confirmed by immunofluorescence, qPCR analysis and immunoblotting (Figures 5a–c). Treatment with control siRNA did not affect vCT differentiation; these cells readily fused into multinuclear structures by 72 h and displayed E-cadherin reorganization (Figure 5a). Contrary to this, silencing of ADAM12 resulted in profound intercellular retention of E-cadherin (Figure 5a). Loss of ADAM12 led to a reduction in the proportion of multinucleated structures (≥ 3 nuclei per cell: A12i5 median = 14.3%, IQR = 5.0–16.9; A12i8 median = 12.3%, IQR = 0.0–19.9; NS median = 37.1%, IQR = 31.8–46.2) (Figure 5d). Consistent with this, multinuclear structures containing 6–9 or ≥ 10 nuclei were not observed in ADAM12-silenced cells, but were readily observed in control siRNA-transfected trophoblasts (Figure 5e). Interestingly, these morphological changes where not reflected by alterations in expression of the fusogenic genes *GCM1* or *ERVW1*, and the expression of the differentiation marker, *CGB* (βhCG), also remained unchanged (Figure 5f). These findings suggest that ADAM12 acts independently of key fusogenic pathways, but is in itself necessary for trophoblast fusion.

ADAM12S overexpression affects intercellular boundaries and potentiates trophoblast fusion. Our observation that ADAM12S is the predominant isoform expressed during vCT and Bewo differentiation indicates a distinct role for ADAM12S in trophoblast fusion. Thus, the importance of ADAM12S was examined in Bewo cells using an ADAM12S overexpression system. Immunofluorescence imaging of ADAM12 revealed it to be perinuclear and cytoplasmic; Bewo cells stably transfected with the empty expression construct, pCMV6, served as a control (Figure 6a). Interestingly, the assessment of E-cadherin showed that intercellular borders were altered in ADAM12S-expressing cells (Figure 6a). Specifically, ectopic ADAM12S led to the disorganization of E-cadherin adhesions characterized by diffuse and poorly defined cell boundaries; PKA stimulation accentuated this phenotype (Figure 6b). Although F/I treatment induced Bewo cell differentiation in control pCMV6 cells, the extent of intercellular disorganization was more pronounced in ADAM12S cells. Importantly, ADAM12S expression increased baseline and forskolin-induced cell fusion over pCMV6 controls (baseline median = 9.9%, IQR = 8.2–11.9 *versus* 2.8%, IQR = 1.1–4.2; F/I = 27.0%, IQR = 25.2–45.2

Figure 3 cAMP-triggered cell fusion in trophoblasts drives ADAM12 expression. (**a**) Representative immunofluorescence images of Bewo cells (from *N* = 6 experiments) probed with antibodies directed against ADAM12 (green) and E-cadherin (Ecad; red) following 0 and 72 h of culture in the absence (NT) or presence of cAMP. DAPI-stained nuclei are labeled blue and dotted white line outlines multi-nucleated syncytial-like structures. Bar = 50 μm. qPCR analysis of (**b**) *ADAM12*L and *ADAM12*S and (**c**) *CDH1* (E-cadherin) and *ERVW1* mRNA transcripts in Bewo cells cultured in 1.0 mM cAMP over 72 h. *GAPDH* was used for normalization. (**d**) Representative immunoblots (*N* = 4) showing ADAM12, E-cadherin and PLAP protein levels in whole cell lysates derived from Bewo cells treated with cAMP over 72 h. Molecular weights (kDa) are shown to the left and GAPDH indicates loading control. Mature ADAM12 (A12) (68 kDa) is indicated. (**e**) qPCR analysis of *ADAM12*L and *ADAM12*S in non-fusogenic JEG-3 and fusogenic Bewo cells left untreated (NT) or treated with cAMP for 48 h. Gene expression experiments were performed in triplicate and replicated *N* = 4 times. (**f**) Representative immunofluorescence images of vCTs probed with antibodies against ADAM12 (green) and E-cadherin (Ecad; red) following 0 and 72 h of culture in forskolin/IBMX (F/I) or DMSO. DAPI-stained nuclei are labeled blue and dotted white line outlines multi-nucleated structures. Bar = 50 μm. Quantification of (**g**) multi-nuclear cells (≥ 3 nuclei per cell) and (**h**) the proportion of multinucleated cells containing 3–5 nuclei, 6–9 nuclei, or ≥ 10 nuclei; box-plots depict the medians and IQRs of proportions of multinucleated vCTs treated with DMSO or with F/I over 72 h. Results are derived from three independent experiments from primary vCTs purified from three distinct plancetae (*N* = 3). (**i**) qPCR analysis of *ADAM12*L and *ADAM12*S in vCTs treated with F/I or DMSO over 72 h. Gene expression experiments were performed in triplicate and replicated *N* = 3 times. qPCR results are presented as mean ± s.e.m. in bar graphs. (**j**) Representative immunoblot (*N* = 3) showing ADAM12 protein levels in whole cell lysates derived from vCTs cells treated with F/I or DMSO over 72 h. Perforated black lines indicate samples run on same blot where lanes were not adjacent to eachother. Molecular weights (kDa) are shown to the left and GAPDH indicates loading control. *$P \leq 0.05$ or **$P \leq 0.01$

versus 19.7%, IQR = 14.5–23.5; Figure 6c). In unstimulated conditions, ADAM12S overexpression also increased the proportion of multinucleated cells containing 3–5 nuclei (ADAM12S median = 9.9%, IQR = 8.8–11.3; pCMV6 median = 2.8%, IQR = 1.1–4.2) and 6–9 nuclei (ADAM12S median = 1.2%, IQR = 0.0–1.7; pCMV6 median = 0.0%, IQR = 0.0-0.0) (Figure 6d). In ADAM12S cells, F/I treatment accentuated fusion, and this was reflected by increased proportions of cells containing 6–9 nuclei (ADAM12S median = 8.9%, IQR = 7.3–12.4; pCMV6 median = 3.8%, IQR = 2.5–5.2) (Figure 6d). In contrast to ADAM12-silenced cytotrophoblasts, ectopic ADAM12S modestly induced transcriptional programs of cell fusion (GCM1, ERVW1), but had no effect on CGB expression (Figure 6e). These findings indicate that cell fusion machinery is enhanced in ADAM12S overexpressing cells.

Disruption of E-cadherin in ADAM12S-expressing Bewo cells suggests involvement of proteolytic shedding. To assess this possibility, we assayed conditioned media (CM) and whole cell lysates from pCMV6 and ADAM12S transfected cells for ADAM12 and E-cadherin. As expected, pro- and mature-ADAM12S protein species were detectable in CM of ADAM12S-expressing cells and undetectable in pCMV6 controls (Figure 6f). Consistent with our previous findings, F/I treatment increased ADAM12 in CM of pCMV6 controls. Interestingly, F/I treatment increased ADAM12S expression over baseline levels in ADAM12S-transfected cells, and we reasoned that this increase may be due to the cAMP

responsive element (CRE) within the CMV promoter[30] (Figure 6f). Importantly, ectopic ADAM12S led to an increase in soluble (85 kDa) E-cadherin (Figure 6f). Upon F/I treatment, soluble E-cadherin was further increased, and this was observed in control and ADAM12S-expressing cells, signifying that PKA activates both ADAM12-dependent and -independent E-cadherin shedding events. Nonetheless, these observations indicate that ADAM12S promotes trophoblast fusion through ectodomain cleavage of E-cadherin.

ADAM12-directed ectodomain shedding of E-cadherin necessitates intrinsic catalytic activity. To test whether ADAM12S-directed proteolysis directs ectodomain shedding of E-cadherin, we treated Bewo cells expressing ADAM12S with either TAPI-1 or TAPI-2, two broad-spectrum metalloprotease/ADAM inhibitors. TAPI-1 and TAPI-2 treatment inhibited ADAM12S-mediated cleavage of E-cadherin, as shown by reduced soluble 85 kDa E-cadherin in CM (Figure 7a). This was supported by immunofluorescence imaging, where ADAM12S-directed disruption of E-cadherin was rescued by TAPI-2 (Figure 7b). Overexpression of ADAM12S harboring a point mutation within its catalytic domain rendering it inactive (ADAM12S$^{\Delta E351Q}$)[18,31] also rescued E-cadherin shedding (Figures 7c and d). Importantly, the proportion of fused cells was significantly lower in ADAM12S$^{\Delta E351Q}$ cells than in ADAM12S cells (Figure 7e). Evidence that ADAM12S cleaves E-cadherin was demonstrated by an in vitro ADAM12 cleavage assay. ADAM12S,
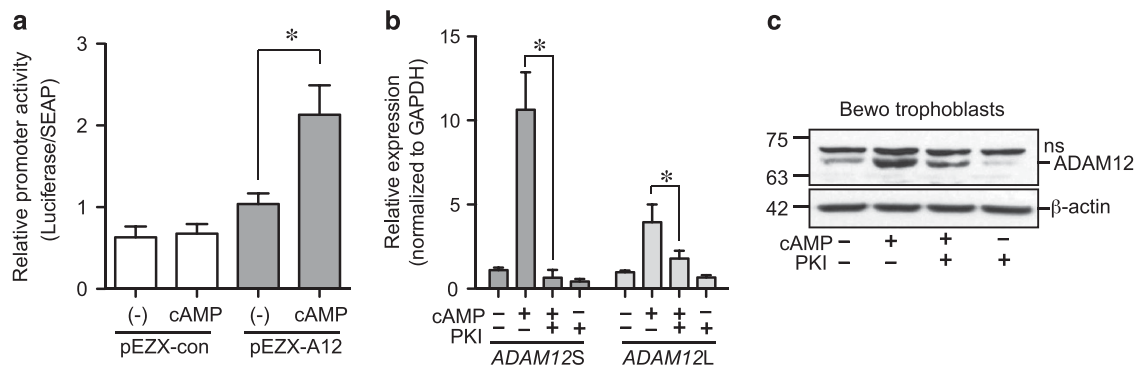
Figure 4 PKA controls ADAM12 gene expression in trophoblasts. (**a**) Bar graphs show quantification of ADAM12 promoter activity in non-treated (−) and cAMP-treated Bewo cells. Cells were transiently transfected with an empty pEZX-con or pEZX-ADAM12 promoter reporter luciferase vector. After 24 h of cAMP treatment, the luminescence of conditioned medium was measured. (**b**) qPCR analysis of ADAM12S and ADAM12L in Bewo cells left untreated or treated in combination with cAMP and the PKA-inhibitor PKI over 48 h. GAPDH was used for normalization. (**c**) Representative immunoblots (N = 3) showing ADAM12 in whole cell lysates of Bewo cells left untreated or treated in combination with cAMP and the PKA-inhibitor PKI over 48 h. β-actin indicates loading control. Promoter activity and gene expression assays were performed in triplicate and repeated N = 3 times. The results are presented as mean ± s.e.m; *P ≤ 0.05 compared with untreated (−) control

Figure 5 ADAM12 deficiency blocks spontaneous cytotrophoblast fusion. (**a**) Representative immunofluorescence images (from N = 4 experiments) of vCTs probed with antibodies directed against ADAM12 (green) and E-cadherin (Ecad; red). Cell were untreated (−) or transfected with non-silencing (NS) or ADAM12-targeting siRNAs (A12i5, A12i8) and cultured for 24 or 72 h. DAPI-stained nuclei are labeled blue. Perforated white box shows magnified region while dotted line outlines multi-nucleated syncytial-like cell structures. Bar = 50 μm. (**b**) qPCR analysis of ADAM12L (A12L) and ADAM12S (A12S) in NS and ADAM12 siRNA-transfected cells. GAPDH was used for normalization. (**c**) Immunoblot showing protein levels of ADAM12 in cell lysates from cytotrophoblasts transfected with control (NS) or ADAM12-directed siRNAs and cultured for 72 h. Molecular weights (kDa) are shown to the left and GAPDH indicates loading control. Box-plots represent quantification of the proportion of (**d**) multinucleated cytotrophoblasts (≥ 3 nuclei per cell) or (**e**) multinucleated cells containing 3–5 nuclei, 6–9 nuclei or ≥ 10 nuclei in cultures untreated (24 h) or transfected with NS or ADAM12-directed siRNAs (72 h). Medians are denoted by solid black lines, while top and bottom box edges denote first and third quartiles. Whiskers show the largest and smallest data point within 1.5 times the IQR. (**f**) qPCR analysis of GCM1, ERVW1 and CGB (βhCG) in siRNA-transfected cytotrophoblasts cultured over 48 h. Gene expression was performed in triplicate on primary cytotrophoblasts isolated from four distinct term placentae (N = 4). GAPDH was used for normalization; qPCR data presented as mean ± s.e.m. *P ≤ 0.05 or **P ≤ 0.01 compared with untreated NS control
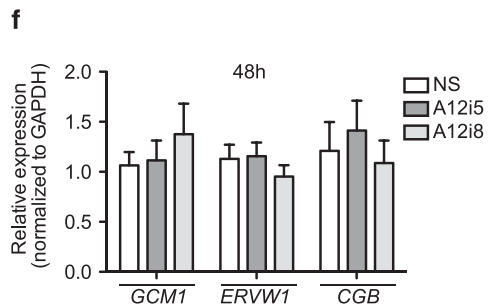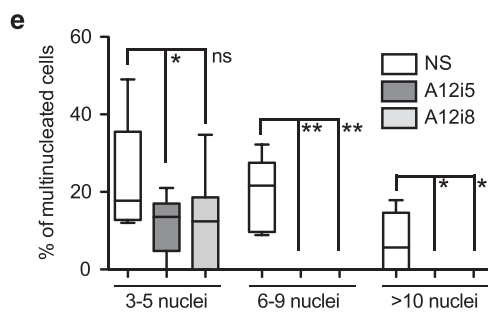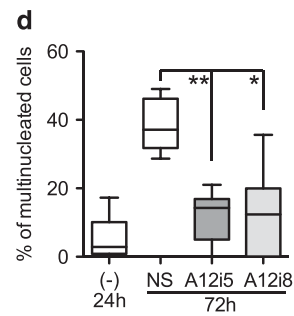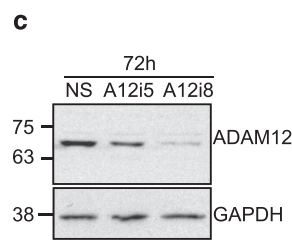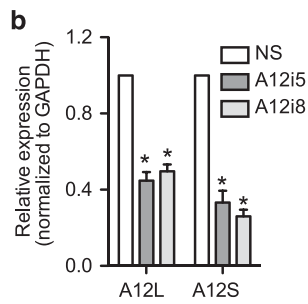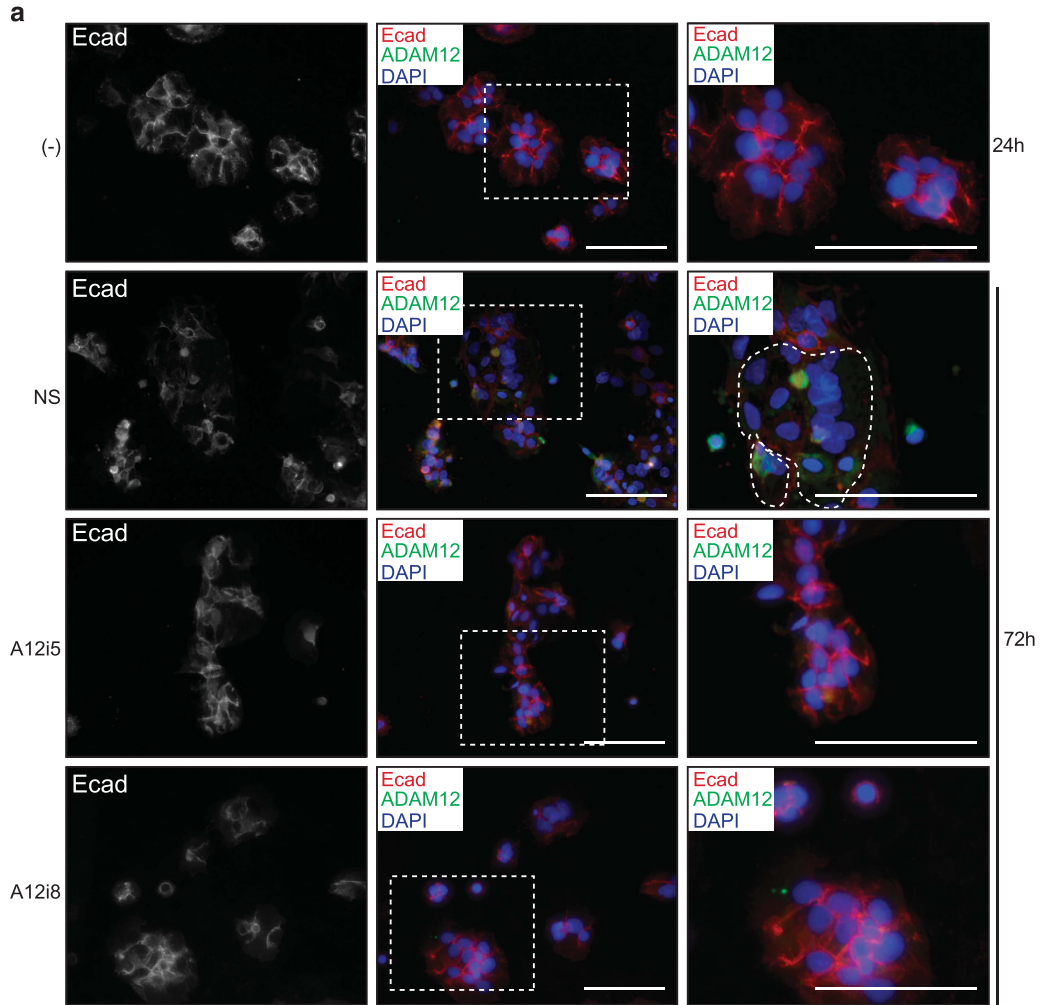
purified from whole cell lysate of ADAM12S-GFP expressing cells by GFP immunoprecipitation, was incubated with recombinant E-cadherin; in this experiment, purified ADAM12S$^{\Delta E351Q}$-GFP and GFP served as a controls. ADAM12S-GFP generated a 110 kDa E-cadherin cleavage product, shown by immunoblotting against E-cadherin, whereas neither ADAM12S$^{\Delta E351Q}$-GFP nor GFP generated cleaved E-cadherin products (Figure 7f). Collectively, these data show that ADAM12S cleaves E-cadherin's ectodomain, disrupts intercellular boundaries and promotes trophoblast fusion.

Cytotrophoblast E-cadherin integrity is controlled by ADAM12. To test whether physiological levels of ADAM12 direct E-cadherin cleavage, we examined whether ADAM12 knockdown affects soluble E-cadherin in vCTs. CM harvested 48 h post siRNA transfection (NS and ADAM12-specific siRNA) was assayed for E-cadherin by immunoprecipitation. Soluble E-cadherin was detectable in CM of control (NS) cytotrophoblasts, while ADAM12-targeting reduced amounts of soluble E-cadherin, suggesting that as in Bewo cells, ADAM12 cleaves the extracellular domain of E-cadherin (Figure 8a). Fluorescence imaging of ADAM12 and E-cadherin verified ADAM12 siRNA-directed knockdown, and re-affirmed that ADAM12 siRNA depletion blocks intercellular disorganization (Figure 8b).

E-cadherin transcription is dynamically downregulated in fusing vCTs.[14] To test the possibility that ADAM12 alterations might impact E-cadherin expression, we examined E-cadherin mRNA levels in control (NS) and ADAM12 siRNA-transfected vCTs. qPCR analysis showed that ADAM12 loss did not alter E-cadherin (*CDH1*) expression (Figure 8c). To demonstrate that E-cadherin cleavage in fusing trophoblasts is primarily attributable to ADAM12, and not to related ADAM proteases known to cleave E-cadherin (i.e. ADAM10 and ADAM15),[32,33] we examined the expression of these proteases. qPCR analysis of *ADAM10* and *ADAM15* over 72 h showed that their levels actually decreased, an observation opposite to the expression of *ADAM12* (Figure 8d). These findings suggest that ADAM12 is the dominant ADAM protease capable of cleaving E-cadherin in differentiating trophoblasts.

Lastly, we immunostained sections of first trimester placenta with antibodies targeting E-cadherin and ADAM12; visualization of trophoblast subtypes is shown by HLA-G and KRT7 labeling. Interestingly, ADAM12 positivity was observed in select E-cadherin-positive vCTs, where its signal appeared perinuclear and proximal to E-cadherin intercellular boundaries (Figure 8e). Notably, intense ADAM12 expression was localized to vCTs fusing with overlying synCT, providing *in vivo* evidence that ADAM12 expression during vCT differentiation participates in E-cadherin remodeling at cell–cell boundaries (Figure 8e).

Discussion

Here, we describe a novel role for ADAM12 in controlling trophoblast fusion. We show that suppression of ADAM12 in primary cytotrophoblasts inhibits cell fusion, whereas ectopic expression potentiates fusion by promoting intercellular remodeling and disorganization of adherens junctions. We

provide evidence that ADAM12S contributes to vCT fusion through ectodomain shedding of E-cadherin. This is the first report demonstrating a functional role for ADAM12 in directing trophoblast fusion, and in addition highlights a novel ADAM12 substrate.

Cell fusion is fundamental to multiple cellular processes, including the immune response, tissue homeostasis and regeneration, and possibly cancer.[3] The molecular processes important in cell fusion have been primarily identified from studies examining intracellular vesicle fusion and viral–host cell fusion.[34] In these systems, fusogenic molecules can be grouped into three types: (i) molecules that facilitate cell–cell adhesion; (ii) molecules that directly rearrange cell lipid bilayers and promote fusion pore formation; and (iii) molecules that direct fusion pore extension and complete membrane disassembly.[3] The importance of ADAM proteins in sperm–egg and myoblast fusion appears to be related to their abilities to affect the initial stages of cell–cell adhesion (i.e. ADAMs may be type-1 fusion proteins). Specifically, the disintegrin domain of ADAM2 directs sperm–egg adhesion via $\alpha6\beta1$ integrin,[35] while ADAM12-$\alpha9\beta1$ integrin promotes myoblast fusion in muscle.[36] In our work, ADAM12 is dynamically increased in differentiating cytotrophoblasts and promotes E-cadherin shedding. This molecular process appears to be important for cell fusion because siRNA depletion of ADAM12 severely dampens E-cadherin ectodomain shedding as well as syncytial formation, and this occurs irrespective of fusogenic gene regulation (i.e. *GCM1*/*ERVW1*). In this respect, ADAM12 impacts cell adhesion as well as cell fusion, but whether it affects the initial stages of cell–cell adhesion prior to fusion or during membrane disassembly is difficult to decipher.

Whether ADAM12 functions as a bonafide sheddase or potentiates the activity of other proteases capable of cleaving E-cadherin necessitates further investigation. It was shown that ADAM12L controls MMP14 activity through an $\alpha v\beta3$ integrin-dependent mechanism independent of its cytoplasmic tail or catalytic activity.[37] Similarly, ADAM12S may control the activity of E-cadherin sheddases like MMP14; however, our demonstration that ADAM12's catalytic activity is required for E-cadherin shedding, combined with findings showing that ADAM12 directly cleaves several membrane-bound substrates, including the type-II cadherin VE-cadherin,[38] supports a role for direct proteolysis of E-cadherin by ADAM12.

Discrepancies exist related to ADAM12 expression within the placenta, where previous studies have localized ADAM12 to the apical membrane[20,22,39] and cytoplasm[22] of the synCT, as well as stochastically within vCTs.[22] Further, we[20] and others[21] have localized ADAM12 to EVTs; together these data show that ADAM12 is expressed by multiple trophoblast subtypes and imply that ADAM12 has diverse functions in placentation. In this study, FACS purification followed by gene expression analysis of *ADAM12*L and *ADAM12*S in vCTs and column EVTs clearly shows that *ADAM12*S is restricted to EVTs, while *ADAM12*L levels are less defined between these cell types. Further studies are needed to dissect the role of ADAM12L in trophoblast biology.

Our finding that ADAM12 generates a soluble E-cadherin product suggests some interesting possibilities for E-cadherin
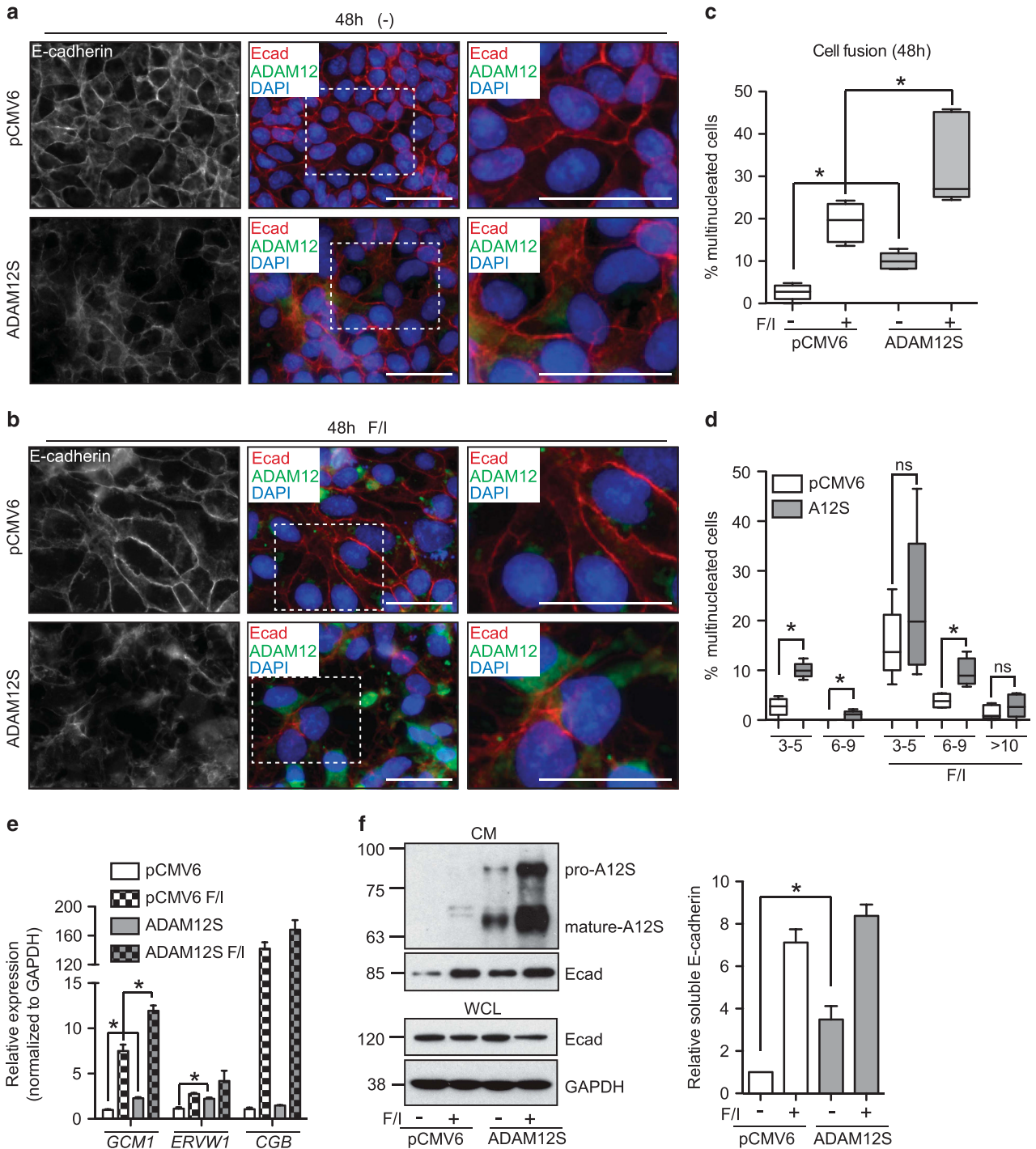
Figure 6 ADAM12S overexpression potentiates trophoblastic cell fusion. (**a**) Representative immunofluorescence images (from $N=6$ experiments) of stably transfected Bewo cells probed with antibodies directed against ADAM12 (green) and E-cadherin (Ecad; red). Cells were transfected with pCMV6 or pCMV6-ADAM12S (ADAM12S) expression constructs and cultured for 48 h after seeding; DAPI-stained nuclei are labeled blue. Perforated white box shows magnified region. (**b**) As above, except Bewo cells are treated with forskolin/IBMX (F/I). Bar = 50 μm. Quantification of (**c**) multi-nuclear cells (≥ 3 nuclei per cell) in (**a**) and (**b**) and (**d**) the proportion of multinucleated cells containing 3–5 nuclei, 6–9 nuclei or ≥ 10 nuclei; box-plots depict the medians and IQRs of proportions of multinucleated Bewo cells stably transfected with pCMV6 or ADAM12S expression constructs. (**e**) qPCR analysis of *GCM1*, *ERVW1* and *CGB* (βhCG) in F/I-stimulated Bewo cells stably transfected with the control pCMV6 or ADAM12S expression constructs. Gene expression was performed in triplicate on three independent occasions ($N=3$); data presented as mean $\pm$ s.e.m. (**f**) Representative immunoblot ($N=4$) showing ADAM12 and E-cadherin (Ecad) protein levels in CM or whole cell lysates from Bewo cells stably transfected with pCMV6 or ADAM12S. Molecular weights (kDa) are shown to the left, pro- and mature-ADAM12S (A12S) are shown on the right and GAPDH indicates loading control. Quantification of soluble 85 kDa E-cadherin from CM of above indicated cells is shown to the right; data presented as mean $\pm$ s.e.m. *$P \leq 0.05$; **$P \leq 0.01$; ns = not significant
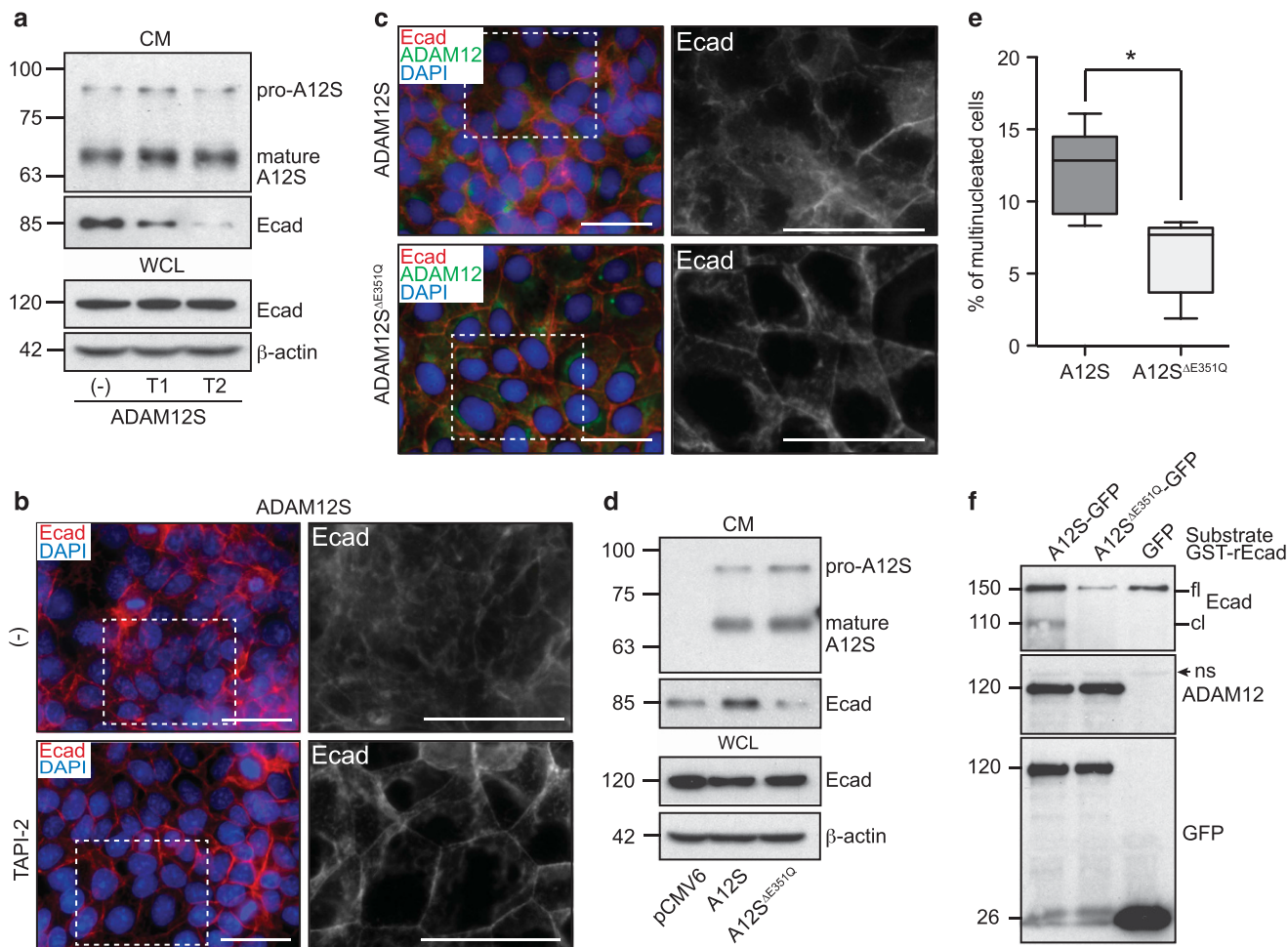
Figure 7 ADAM12S controls trophoblast fusion in part by E-cadherin ectodomain shedding. (**a**) Representative immunoblots ($N = 3$) of CM or whole cell lysates (WCL) from ADAM12S-transfected Bewo cells cultured for 72 h in the absence ($-$) or presence of the broad-spectrum metalloproteinase inhibitors, TAPI-1 (T1) or TAPI-2 (T2). Lysates were probed with antibodies directed against ADAM12 (pro-A12S; mature-A12S) or E-cadherin (Ecad). Molecular weights (kDa) are shown to the left and β-actin indicate loading controls. (**b**) Representative immunofluorescence images ($N = 3$) of ADAM12S-transfected Bewo cells probed with anti-E-cadherin antibody (Ecad; red). Cells were either untreated ($-$) or cultured in the presence of TAPI-2; DAPI-stained nuclei are labeled blue. White perforated box indicates magnified area. (**c**) ADAM12 (green) and E-cadherin (Ecad; red) immunofluorescence images of Bewo cells stably transfected with either wildtype ADAM12S or protease-dead ADAM12S$^{\Delta E351Q}$ expression constructs; Bars $= 50\ \mu$m. (**d**) Immunoblots ($N = 3$) of ADAM12S and E-cadherin in CM or WCL of Bewo cells stably transfected with the control pCMV6 construct as well as expression constructs described in (**c**). Molecular weights (kDa) are shown to the left and β-actin indicates loading control. (**e**) Box-plots depicting median and IQR values of the percent of multi-nucleated cells in ADAM12S and ADAM12S$^{\Delta E351Q}$ Bewo cells ($N = 3$) cultured over 72 h; *$P \leq 0.05$. (**f**) Representative immunoblots ($N = 3$) probed with antibodies directed against E-cadherin (Ecad), GFP and ADAM12 showing ADAM12-directed E-cadherin cleavage. Immunoprecipitated ADAM12-GFP was incubated with recombinant GST N-tagged E-cadherin (GST-rEcad); immunoprecipitated GFP and ADAM12$^{\Delta E351Q}$-GFP serve as controls. The full-length (fl) and cleaved (cl) E-cadherin products are indicated; ns denotes non-specific bands. Molecular weights (kDa) are shown to the left

shedding in cell fusion. Firstly, the E-cadherin ectodomain may impart molecular cues required for cell fusion. This possibility is supported by recent findings showing that ADAM10- and ADAM15-cleaved E-cadherin activates multiple pathways (EGFR/IGFR), drives MMP activity and promotes tumor cell invasion;[40,41] these pathways are also important in trophoblast fusion, highlighting a possible function for the E-cadherin ectodomain during syncytialization.[42,43] Secondly, ADAM10-directed ectodomain shedding of E-cadherin and N-cadherin promotes β-catenin nuclear localization and activates Wnt/β-catenin signaling pathways.[32,33] The transcription factor, GCM1, which is central in trophoblast fusion, is a downstream target of Wnt/β-catenin, suggesting that proteolytic events controlling E-cadherin cleavage and β-catenin activation may also regulate trophoblast fusion.[44] This possibility is supported

by our findings that ADAM12S overexpression leads to increases in both *GCM1* and *ERVW1* expression, supporting the likelihood that ADAM12 regulates *GCM1* through an E-cadherin-dependent mechanism.

In summary, this study defines a novel role for ADAM12 in trophoblast fusion. The diverse functions of ADAM12 in placental development are beginning to be elucidated: its roles in promoting trophoblast invasion and fusion have now been defined. Notably, ADAM12S, which shows restricted expression in normal adult tissues, appears to be a key protease in placentation. Future work aimed at characterizing the precise molecular events following ADAM12-directed E-cadherin cleavage will provide needed insight into the cellular mechanisms governing trophoblast fusion and may shed light on the importance of ADAM12-directed ectodomain
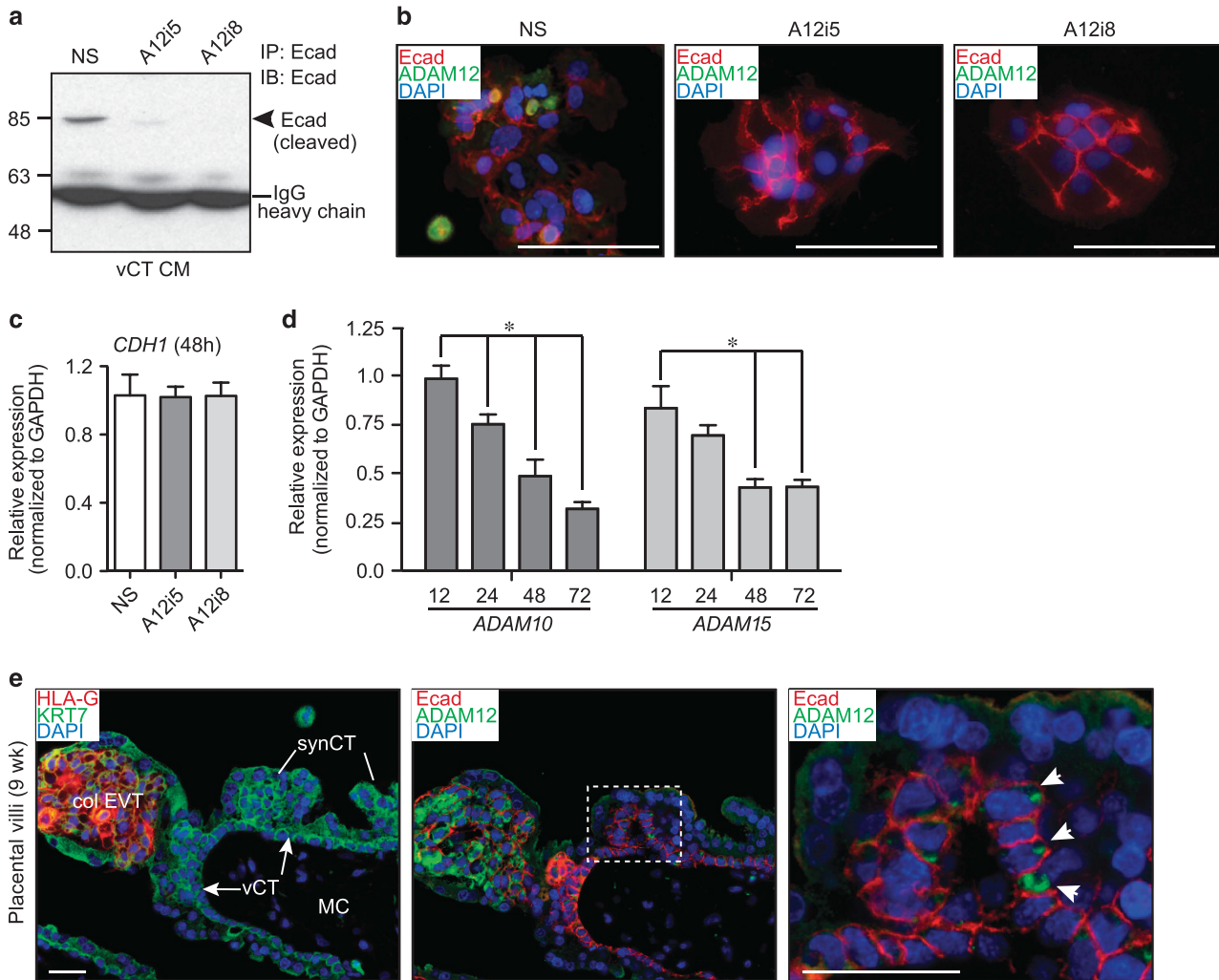
Figure 8 ADAM12 participates in E-cadherin-directed intercellular junction remodeling during cytotrophoblast fusion. (**a**) Representative immunoblot of E-cadherin protein immunoprecipitated from CM derived from villous cytotrophoblast cultures (vCT CM) transfected with non-silencing control siRNA (NS) or siRNAs targeting ADAM12 (A12i5 and A12i8). Immunoprecipitated protein was subsequently immunoblotted using an antibody directed against the extracellular domain of E-cadherin. The IgG heavy chain is indicated, while protein loading is normalized by Ponceau staining. Molecular weights (kDa) are shown to the left. (**b**) Immunofluorescence images of siRNA-transfected cytotrophoblasts (as above) probed with antibodies directed against E-cadherin (Ecad; red) and ADAM12 (green); DAPI-stained nuclei are labeled blue. Cells were allowed to differentiate for 72 h post seeding. Images are representative of three independent experiments ($N = 3$). (**c**) qPCR analysis of *CDH1* in spontaneously fusing vCTs at 48 h of culture. Gene expression experiments were performed in triplicate and repeated on cells isolated from three distinct placentae ($N = 3$). (**d**) qPCR analysis of *ADAM10* and *ADAM15* mRNA transcripts in differentiating primary cytotrophoblasts cultured over 72 h. *GAPDH* was used for normalization. Gene expression experiments were performed in triplicate and repeated on cells isolated from three distinct placentae ($N = 3$). Data presented as mean ± s.e.m; *$P \leq 0.05$. (**e**) Representative images of 9 week gestation first trimester placental villi ($N = 5$ placental villi) immunostained for HLA-G (red), KRT7 (green), E-cadherin (Ecad; red) and ADAM12 (green). Nuclei are labeled with DAPI (blue). Column EVTs (col EVT), vCTs, synCT and mesenchymal core cells (MC) are indicated. Perforated box shows area of image magnification to right. White arrowheads indicate E-cadherin positivity in vCTs differentiating into synCT. Bars = 50 μm

shedding of cell adhesion molecules in other physiological and pathological processes.

Materials and Methods

Tissues, cytotrophoblast isolation and cell culture. Human placental tissues were obtained with approval from the Research Ethics Board on the use of human subjects, University of British Columbia. All women provided informed written consent.

First trimester placental tissues ($N = 14$) were obtained from women undergoing elective termination of pregnancy (gestational ages ranging from 5 to 12 weeks). Term placentae ($N = 5$) were obtained from healthy women undergoing elective Caesarian section at 38 weeks gestation. vCTs were isolated from term placental tissues using an adapted procedure derived by Kliman *et al.*[29] Following multiple

washes in sterile ice-cold saline, 100 g of finely minced placental tissue was subjected to two 30-min digestions in a 37 °C shaking incubator; the digestion cocktail (200 ml) consisted of Hank's Balanced Salt Solution/HEPES in 250 μg trypsin (Sigma, St. Louis, MO, USA; T8003), 250 μg DNase I (Sigma; DN25) and 5 IU dispase (Thermo Fisher Scientific, Waltham, MA, USA; CB-40235). Single cells obtained after digestion were subjected to a discontinuous (10–70%) Percoll gradient centrifugation that yielded highly enriched preparations (>90%) of mononucleate cytotrophoblasts as determined by cytokeratin-7 and vimentin fluorescence microscopy. Following isolation, cells were cultured in phenol-red free DMEM/F12 medium (Invitrogen, Carlsbad, CA, USA) containing 25 mM glucose, 25 mM HEPES, 1× Anti anti-mycotic (Gibco, Grand Island, NE, USA), 100 IU/ml penicillin/streptomycin (Gibco) and supplemented with 10% fetal bovine serum (Gibco).

Bewo choriocarcinoma cells (B30 clone, which fuse upon treatment with forskolin or cAMP) kindly gifted by Jerome Strauss III were maintained in Ham's F12 (Kaighn's)

medium (Invitrogen) containing 25 mM glucose, L-glutamine, 100 IU/ml penicillin/streptomycin and supplemented with 10% FBS. For differentiation studies examining cell fusion, Bewo cells were cultured in the presence or absence of 1.0 mM 8-bromoadenosine-3' 5'-cyclic monophosphate sodium salt (8-Br-cAMP; Sigma) or 25 μM forskolin (Sigma)/100 μM IBMX (Sigma) over 72 h. In PKA inhibition experiments, 20 μM PKI (Promega, Madison, WI, USA) was pre-incubated in Bewo cultures for 1 h prior to PKI/cAMP co-treatments. The broad-spectrum metalloproteinase inhibitors, TAPI-1 (10 μM; Enzo Life Sciences, Farmingdale, NY, USA) and TAPI-2 (10 μM; Enzo Life Sciences), were added to culture media in select experiments; 0.5% DMSO was added to control cells. JEG-3 trophoblastic cells were purchased from (ATCC; Manassas, VA, USA) and were cultured in DMEM media containing 25 mM glucose, L-glutamine, antibiotics (100 U/ml penicillin, 100 μg/ml streptomycin) and supplemented with 10% FBS.

Immunohistochemistry and immunofluorescence microscopy. Placental villi (6–12 weeks gestation; $N = 10$) were fixed in 2% paraformaldehyde overnight at 4 °C. vCT cultures or Bewo cells were fixed in 4% paraformaldehyde for 20 min at 4 °C, followed by washing and storage in PBS. Tissues were paraffin-embedded and sectioned at 5 μm onto glass slides. Immunofluorescence was performed as described elsewhere.[20] Briefly, cells or placental tissues underwent antigen retrieval by heating slides in a microwave for 5 × 2 min intervals in a citrate buffer (pH 6.0). Sections were incubated with sodium borohydride for 5 min, RT, followed by Triton X-100 permeabilization for 5 min, RT. Slides were blocked in 5% normal goat serum/0.1% saponin for 1 h, RT, and incubated with combinations of the indicated antibodies overnight, 4 °C; rabbit polyclonal ADAM12 (1 : 50, ProteinTech, Chicago, IL, USA), mouse monoclonal KRT7 (1 : 100, clone RCK105, Santa Cruz Biotechnologies, Dallas, TX, USA); rabbit monoclonal KRT7 (1 : 75, clone SP52, Ventana Medical Systems, Tucson, AZ, USA), mouse monoclonal E-cadherin (1 : 400, clone 36, BD, San Diego, CA, USA); mouse monoclonal HAI-1 (1 : 75, clone 4H2, LifeSpan BioSciences, Seattle, WA, USA); mouse monoclonal HLA-G (1 : 100, clone 4H84, Exbio, Vestec, Czech Republic); rabbit monoclonal Ki67 (1 : 100, clone SP6; Thermo Scientific). Slides were incubated with Alexa Fluor goat anti rabbit-568/-488 and goat anti-mouse-568/-488-conjugated secondary antibodies (Life Technologies) for 1 h, RT. Glass coverslips were mounted onto slides using a DAPI mounting media (Life Technologies) and slides were imaged using a ×40/0.75NA objective (Leica DM4000B, Wetzlar, Germany; Figures 2, 3, 5 and 6, and supplementary Figures 1 and 2) or a ×40 oil/1.4NA objective (Carl Zeiss Axio Observer, Oberkochen, Germany; Figures 1 and 8) fluorescence microscopes. Images in Figure 1 were obtained by multiple Z-stacks (90 stacks; 0.24 μm optical sections) and subjected to iterative maximum likelihood algorithm deconvolution (ZenPro software, Oberkochen, Germany); representative reconstructed images are shown as maximum intensity projections.

FACS purification of placental cells. Placental villi single cell suspensions were generated from fresh first trimester placental specimens ($N = 4$) by enzymatic digestion and analyzed by flow cytometry following protocols adapted from Joshi *et al.*[45] and Beristain *et al.*[46] Briefly, placental villi were digested for 1.5 h at 37 °C in Hank's Balanced Salt Solution, 750 U/ml collagenase and 250 U/ml hyaluronidase. Organoids obtained after vortexing were subjected to red blood cell lysis in 0.8% NH4Cl, further dissociation in 0.25% trypsin for 2 min, 5 mg/ml dispase with 0.1 mg/ml DNase I for 2 min, and filtered through a 40 μm mesh to obtain single cells. Contaminating immune and endothelial cells were removed from the cell admixture by EasySep immuno-magnetic bead purification (all reagents obtained from StemCell Technologies Inc, Vancouver, BC, Canada). Following magnetic bead exclusion, 2.5×10^6 cells were blocked with Fc receptor antibody (eBioscience, San Diego, CA, USA), and incubated with the following antibodies on ice for 30 min: anti-CD45 (clone 2D1, eBioscience), anti- CD49f-PE-Cy7 (clone GoH3, eBioscience) and anti- HLA-G-PE (clone 87G, eBioscience). Dead cells were excluded from analysis by staining with 7AAD (eBioscience). The cell surface markers CD49f and HLA-G were used to identify placental trophoblast cell populations, while CD45 was used to identify and exclude contaminating immune cells that were not completely removed by EasySep magnet purification. FACS analysis was performed using FACSDiva (BD) and FlowJo software (Tree Star, Inc. Ashland, OR, USA). Cell sorting was performed on a FACSAria (BD) into tubes containing ice-cold Hank's Balanced Salt Solution/2% FBS.

Gene expression analysis. Total RNA was prepared from placental villi or cell lines using TRIzol (Life Technologies). Total RNA was prepared from FACS-sorted primary placental cell subpopulations using the PicoPure RNA Isolation Kit

(Agilent Technologies, Santa Clara, CA, USA) as described in Beristain *et al.*[46] RNA purity was confirmed using a NanoDrop Spectrophotometer (Thermo Fisher Scientific) and by running RNA on formaldehyde agarose gels to observe the integrity of 18 S and 28 S ribosomal RNA species. One microgram of RNA was reverse-transcribed using a first-strand cDNA synthesis kit (QuantaBiosciences Inc.; Gaithersburg, MD, USA) and subjected to qPCR ($\Delta\Delta$CT) analysis, using Perfecta SYBR Green FastMix (QuantaBiosciences) on an ABI 7500 Sequence Detection System (Life Technologies). Forward and reverse primer sets were as follows: *ADAM10* (F: 5'-GGATTGTGGCTCATTGGTGGGCA-3', R: 5'-ACTCTCTCGG GGCCGCTGAC-3'), *ADAM12S* (F: 5'-GTGACAAGTTTGGCTTTGGAG 3', R: 5'-GTGAGGCAGTAGACGCATG-3'), *ADAM12L* (F: 5'-GACAATGGGAGACT GGGC-3', R: 5'-GTGGATCTGGGCACTTGG-3'), *ADAM15* (F: 5'-TGCTGGAAGT CCCGGTAT-3', R: 5'-ACACTCAGAAGCCACCAGA-3'), *CDH1* (E-cadherin) (F: 5'- TGA GTGTCCCCGGTATCTTC-3', R: 5'- CAGTATCAGCCGCTTTCAGATTTT-3'), *ERVW1* (F: 5'- CTTCCTCTCATTCTTAGTGCCC-3', R: 5'- CCAATGCCAGTACCTAGTGC-3'), *GCM1* (F: 5'- GAGGCAAGAAGAGCCATGAA-3', R: 5'- TCTGTGATTCCTCCCAG ACC-3'), *CGB* (βhCG) (F: 5'- GTCAACACCACCATCTGTGC-3', R: 5'- GCACA TTGACAGCTGAGAGC-3'), *VIM* (vimentin) (F: 5'-AAAGTGTGGCTGCCAAGA ACCT-3', R: 5'- ATTTCACGCATCTGGCGTTCCA-3'), *HLA-G* (F: 5'-TTGCT GGCCTGGTTGTCCTT-3', R: 5'-TTGCCACTCAGTCCCACACAG-3'), *KRT7* (cytokerain-7) (F: 5'-GGACATCGAGATCGCCACCT-3', R: 5'- ACCGCCACTGCTACT GCCA-3') and *GAPDH* (F: 5'-AGGGCTGCTTTTAACTCTGGT -3', R: 5'-CCCC ACTTGATTTTGGAGGGA -3'). Primers for *ADAM10*, *ADAM12S*, *ADAM12L*, *CDH1*, *ERVW1*, *GCM1* and *CBG* were previously described.[20,47] All raw data were analyzed using Sequence Detection System software version 2.1 (Life Technologies). The threshold cycle (CT) values were used to calculate relative RNA expression levels. Values were normalized to endogenous *GAPDH* transcripts.

Cell lysis, immunoblot and immunoprecipitation analysis. Cells were washed in ice-cold PBS and incubated either in RIPA cell extraction buffer (20 mM Tris-HCl, pH 7.6, 1% Triton X-100, 0.1% SDS, 1% NP-40, 1% sodium deoxycholate, 5 mM EDTA, 50 mM NaCl) for immunoblot analysis or NP-40 cell extraction buffer (25 mM Tris-HCl, 150 mM NaCl, 1 mM EDTA, 1.0% NP-40, 5% glycerol) for immunoprecipitation analysis; both buffers were supplemented with 10 mM Na$_3$VO$_4$, 10 mM NaF, 2 mM PMSF, and an appropriate dilution of Complete Mini, EDTA-free protease inhibition cocktail tablets (Roche, Nutley, NJ, USA). Protein concentrations were determined using a BCA kit (Thermo Fisher Scientific). For immunoblotting, 30 μg of cell protein lysate was resolved by SDS-PAGE and transferred to nitrocellulose membranes. The membranes were probed using rabbit polyclonal antibodies directed against ADAM12's catalytic domain (ProteinTech; Figures 6 and 7. Abcam, Toronto, ON, Canada; ab28225; Figures 2,3,4,5), PLAP (Abcam, Cambridge, UK; ab118856), or monoclonal antibodies directed against E-cadherin (BD; clone 36 cytoplasmic domain), E-cadherin (Cell Signaling Technologies, Danvers, MA, USA; 32A8 extracellular domain), turbo-GFP (Origene, Rockville, MD, USA) and GST (Cell Signaling Technologies). The blots were stripped and re-probed with an HRP-conjugated monoclonal antibody directed against mouse β-actin (Santa Cruz Biotechnology) or mouse GAPDH (Hytest, Turku, Finland; clone 6C5). In immunoprecipitation experiments, equal volumes of pre-concentrated conditioned medium from cells seeded at 1.5×10^6 cells per plate (via Amicon Ultracel 10 kDa concentrators; Millipore, Darmstadt, Germany) were immunoprecipitated with 0.5 μg anti-E-cadherin antibody (32A8; Cell Signaling Technologies). In E-cadherin cleavage assays (see below), 500 μg of whole cell lysate was immunoprecipitated using 0.5 Log of anti-turbo-GFP antibody. Protein A/G agarose bead conjugation followed by washing in ice-cold 1% NP-40 buffer was used to purify and wash target proteins.

siRNA gene knockdown, expression vectors, site-directed mutagenesis and promoter assays. Two previously published[20] siRNAs (Thermo Scientific; 25 nM) targeting both the ADAM12L and ADAM12S human ADAM12 mRNA transcripts (A12i5 5'-CCAAUGCCGUUUCCAUAGA-3'; A12i8 5'-CAAAUGCUCUGUAAGUCAG-3') were transfected into primary vCTs using Lipofectamine RNAiMAX reagent via a reverse transfection strategy prior to seeding according to manufacturer's protocol (Life Technologies). Cells transfected with ON-TARGETplus non-silencing (NS) siRNA#1 (NS; Cat# D-001810-01-20) or cultured in the presence of transfection reagent alone, served as negative controls.

Full-length human ADAM12S cDNA (GenBank Accession No. NM_021641.3) in the pCMV6-AC or pCMV6-AC-GFP mammalian expression construct backbones were purchased from Origene. Expression constructs pCMV6-AC and pCMV6-AC-GFP served as controls (Origene). Stable transfections were performed to establish

multiclonal Bewo cells constitutively expressing ADAM12S. Two micrograms of plasmid DNA was transfected using Lipofectamine 2000 transfection reagent (Life Technologies) according to the manufacturer's protocol. Selection began 48 h post transfection using 400 μg/ml G418 sulfate in Ham's F-12 medium; after selection, cells were maintained in medium containing 100 μg/ml G418 sulfate.

The generation of the ADAM12S catalytically inactive mutant expression construct, ADAM12S$^{\Delta E351Q}$, was previously described.[20] Briefly, a point mutation in the metalloproteinase domain of ADAM12S was introduced using the QuikChange PCR site directed mutagenesis kit (Agilent Technologies), where guanine (1059) was substituted to cytosine, resulting in a translated protein consisting of a glutamine (Q) at amino acid 351 instead of a glutamate (E), thus rendering the protein catalytically inactive.[18,31] The parent pCMV6-ADAM12S construct served as the template for this reaction.

ADAM12 promoter activity was assayed using the pEZX-PG04 luciferase promoter reporter system (GeneCopoeia, Rockville, MD, USA; Cat# HPRM13238-PG04). The promoter reporter construct, containing a 1237-bp ADAM12 promoter sequence inserted upstream of the Gaussia luciferase (GLuc) and secreted alkaline phosphatase reporter genes in the pEZX-PG04 vector (pEZX-A12), was transiently transfected into Bewo cells using Lipofectamine 2000. The ADAM12 promoter fragment comprises the sequence from position − 1036 to +200 relative to the transcription start site (GeneCopoeia). The promoterless vector containing the luciferase reporter genes (pEZX-con; GeneCopoeia Cat# NEG-PG04) served as a control for these studies. After 24 h of culture, cells were treated with or without cAMP (Sigma). GLuc and secreted alkaline phosphatase activities were assayed from the conditioned medium post treatment using a Secrete-Pair Dual Luminescence assay Kit (GeneCopoeia; Cat# SPDA-D010). Luminescence was measured using Victor^{3}V plate reader (Perkin Elmer, Waltham, MA, USA) and reported as the ratios of Gaussia luciferase normalized to secreted alkaline phosphatase.

Cell fusion assays. Cell fusion was quantified in cultures of primary vCTs and Bewo cells by microscopic analysis of E-cadherin at cell–cell boundaries. Briefly, fused cell proportions were calculated as the ratio of the number of nuclei in multinucleated cellular aggregates (≥ 3 nuclei per aggregate) divided by the number of total nuclei per field of view acquired by a ×40 objective. Cells were seeded (8×10^5 cells) in duplicate within 8-well chamber slides (BD Biosciences) and cultured over 72 h. Bewo cells were treated with either cAMP (1.0 mM) or forskolin (25 μM)/IBMX (100 μM) to induce cell differentiation. Cell fusion was defined as at least three nuclei surrounded by a cell membrane as identified by continuous E-cadherin immunofluorescence staining; nuclei were visualized with DAPI quantified using ImageJ software (ITCN plug-in; version 1.6). Five random images were acquired per well, and from these, fused cell proportions were calculated. Quantification of the proportion of multinucleated cell groups based on the number of nuclei per cell was calculated as described above, except data are presented as the proportion of cells containing 3–5, 6–9 or ≥ 10 nuclei.

E-cadherin cleavage assay. Immunoprecipitated ADAM12S-GFP, ADAM12$^{\Delta E351Q}$-GFP or GFP from stably transfected Bewo cells were combined with full-length recombinant E-cadherin N-terminally tagged with GST (GST-E-cadherin); immunoprecipitation was performed using an antibody targeting tGFP (Origene). Briefly, ADAM12S-GFP, ADAM12$^{\Delta E351Q}$-GFP or GFP immunoprecipitated protein was re-suspended in 60 μl cleavage assay buffer (20 mM TrisHCl, pH 7.4), where 20 μl of Protein A/G agarose-ADAM12S-GFP, -ADAM12$^{\Delta E351Q}$-GFP or -GFP complex were incubated with 400 ng of recombinant GST-E-cadherin in 50 μl PBS, pH 7.4 (Novus Biologicals, Oakville, ON, Canada) for 1 h at 37 °C. Following incubation, cleavage reactions were stopped by adding 6× sample buffer (containing βME), boiled for 5 min and centrifuged to collect supernatants. Samples were analyzed by SDS-PAGE followed by immunoblotting using antibodies directed against the extracellular domain of E-cadherin (Cell Signaling Technologies).

Statistical analysis. Primary cytotrophoblast and Bewo cell fusion assays are reported as median values and IQR. Quantitative PCR gene expression, promoter activities and protein densitometry are presented as mean values ± S.E.M. All calculations were carried out using GraphPad Prism software. For single comparisons, Mann-Whitney non-parametric unpaired t-tests were performed. For multiple comparisons, one-way ANOVA non-parametric Kruskal-Wallis analyses, followed by Dunn's post-test were performed. The differences were accepted as significant at $P < 0.05$.

Conflict of Interest

The authors declare no conflict of interest.

Author contributions

AGB designed the research. AGB, MA, KH, SP and WPR performed experiments and analyzed data. AGB, MA and KH wrote the paper. All authors read and approved the manuscript.

1. Pijnenborg R, Vercruysse L, Carter AM. Deep trophoblast invasion and spiral artery remodelling in the placental bed of the chimpanzee. *Placenta* 2011; **32**: 400–408.
2. Avagliano L, Marconi AM, Romagnoli S, Bulfamante GP. Abnormal spiral arteries modification in stillbirths: the role of maternal prepregnancy body mass index. *J Matern Fetal Neonatal Med* 2012; **25**: 2789–2792.
3. Oren-Suissa M, Podbilewicz B. Cell fusion during development. *Trends Cell Biol* 2007; **17**: 537–546.
4. Chaddha V, Viero S, Huppertz B, Kingdom J. Developmental biology of the placenta and the origins of placental insufficiency. *Semin Fetal Neonatal Med* 2004; **9**: 357–369.
5. Pidoux G, Gerbaud P, Dompierre J, Lygren B, Solstad T, Evain-Brion D et al. A PKA-ezrin-connexin 43 signaling complex controls gap junction communication and thereby trophoblast cell fusion. *J Cell Sci* 2014; **127**: 4172–4185.
6. Wice B, Menton D, Geuze H, Schwartz AL. Modulators of cyclic AMP metabolism induce syncytiotrophoblast formation in vitro. *Exp Cell Res* 1990; **186**: 306–316.
7. Baczyk D, Drewlo S, Proctor L, Dunk C, Lye S, Kingdom J. Glial cell missing-1 transcription factor is required for the differentiation of the human trophoblast. *Cell Death Differ* 2009; **16**: 719–727.
8. Frendo J-L, Olivier D, Cheynet V, Blond JL, Bouton O, Vidaud M et al. Direct involvement of HERV-W Env glycoprotein in human trophoblast cell fusion and differentiation. *Mol Cell Biol* 2003; **23**: 3566–3574.
9. Frendo J-L, Cronier L, Bertin G, Guibourdenche J, Vidaud M, Evain-Brion D et al. Involvement of connexin 43 in human trophoblast cell fusion and differentiation. *J Cell Sci* 2003; **116**: 3413–3421.
10. Dunk CE, Gellhaus A, Drewlo S, Baczyk D, Pötgens AJ, Winterhager E et al. The molecular role of connexin 43 in human trophoblast cell fusion. *Biol Reprod* 2012; **86**: 115.
11. Gauster M, Siwetz M, Orendi K, Moser G, Desoye G, Huppertz B. Caspases rather than calpains mediate remodelling of the fodrin skeleton during human placental trophoblast fusion. *Cell Death Differ* 2010; **17**: 336–345.
12. Chang C-W, Chang G-D, Chen H. A novel cyclic AMP/Epac1/CaMKI signaling cascade promotes GCM1 desumoylation and placental cell fusion. *Mol Cell Biol* 2011; **31**: 3820–3831.
13. Getsios S, Maccalman CD. Cadherin-11 modulates the terminal differentiation and fusion of human trophoblastic cells in vitro. *Dev Biol* 2003; **257**: 41–54.
14. Coutifaris C, Kao LC, Sehdev HM, Chin U, Babalola GO, Blaschuk OW et al. E-cadherin expression during the differentiation of human trophoblasts. *Development* 1991; **113**: 767–777.
15. Nishimura T, Takeichi M. Remodeling of the adherens junctions during morphogenesis. *Curr Top Dev Biol* 2009; **89**: 33–54.
16. Blobel CP. ADAMs: key components in EGFR signalling and development. *Nat Rev Mol Cell Biol* 2005; **6**: 32–43.
17. Weber S, Saftig P. Ectodomain shedding and ADAMs in development. *Development* 2012; **139**: 3693–3709.
18. Sahin U, Weskamp G, Kelly K, Zhou HM, Higashiyama S, Peschon J et al. Distinct roles for ADAM10 and ADAM17 in ectodomain shedding of six EGFR ligands. *J Cell Biol* 2004; **164**: 769–779.
19. Iba K, Albrechtsen R, Gilpin B, Fröhlich C, Loechel F, Zolkiewska A et al. The cysteine-rich domain of human ADAM 12 supports cell adhesion through syndecans and triggers signaling events that lead to beta1 integrin-dependent cell spreading. *J Cell Biol* 2000; **149**: 1143–1156.
20. Aghababaei M, Perdu S, Irvine K, Beristain AG. A disintegrin and metalloproteinase 12 (ADAM12) localizes to invasive trophoblast, promotes cell invasion and directs column outgrowth in early placental development. *Mol Hum Reprod* 2014; **20**: 235–249.
21. Biadasiewicz K, Fock V, Dekan S, Proestling K, Velicky P, Haider S et al. Extravillous trophoblast-associated ADAM12 exerts pro-invasive properties, including induction of integrin beta 1-mediated cellular spreading. *Biol Reprod* 2014; **90**: 101.
22. Kokozidou M, Drewlo S, Bartz C, Raven G, Brandenburg LO, Wruck CJ et al. Complex patterns of ADAM12 mRNA and protein splice variants in the human placenta. *Ann Anat* 2011; **193**: 142–148.

23. Verrier S, Hogan A, McKie N, Horton M. ADAM gene expression and regulation during human osteoclast formation. *Bone* 2004; **35**: 34–46.

24. Kurisaki T, Masuda A, Sudo K, Sakagami J, Higashiyama S, Matsuda Y *et al.* Phenotypic analysis of Meltrin alpha (ADAM12)-deficient mice: involvement of Meltrin alpha in adipogenesis and myogenesis. *Mol Cell Biol* 2003; **23**: 55–61.

25. Kveiborg M, Albrechtsen R, Rudkjaer L, Wen G, Damgaard-Pedersen K, Wewer UM *et al.* ADAM12-S stimulates bone growth in transgenic mice by modulating chondrocyte proliferation and maturation. *J Bone Miner Res* 2006; **21**: 1288–1296.

26. Foack V, Mairhofer M, Otti GR, Hiden U, Spittler A, Zeisler H *et al.* Macrophage-derived IL-33 is a critical factor for placental growth. *J Immunol* 2013; **191**: 3734–3743.

27. Damsky CH, Librach C, Lim KH, Fitzgerald ML, McMaster MT, Janatpour M *et al.* Integrin switching regulates normal trophoblast invasion. *Development* 1994; **120**: 3657–3666.

28. Zhou Y, Fisher SJ, Janatpour M, Genbacev O, Dejana E, Wheelock M *et al.* Human cytotrophoblasts adopt a vascular phenotype as they differentiate. A strategy for successful endovascular invasion? *J Clin Invest* 1997; **99**: 2139–2151.

29. Kliman HJ, Nestler JE, Sermasi E, Sanger JM, Strauss JF 3rd. Purification, characterization, and in vitro differentiation of cytotrophoblasts from human term placentae. *Endocrinology* 1986; **118**: 1567–1582.

30. Chang YN, Crawford S, Stall J, Rawlins DR, Jeang KT, Hayward GS. The palindromic series I repeats in the simian cytomegalovirus major immediate-early promoter behave as both strong basal enhancers and cyclic AMP response elements. *J Virol* 1990; **64**: 264–277.

31. Kveiborg M, Fröhlich C, Albrechtsen R, Tischler V, Dietrich N, Holck P *et al.* A role for ADAM12 in breast tumor progression and stromal cell apoptosis. *Cancer Res* 2005; **65**: 4754–4761.

32. Reiss K, Maretzky T, Ludwig A, Tousseyn T, de Strooper B, Hartmann D *et al.* ADAM10 cleavage of N-cadherin and regulation of cell-cell adhesion and beta-catenin nuclear signalling. *EMBO J* 2005; **24**: 742–752.

33. Maretzky T, Reiss K, Ludwig A, Buchholz J, Scholz F, Proksch E *et al.* ADAM10 mediates E-cadherin shedding and regulates epithelial cell-cell adhesion, migration, and beta-catenin translocation. *Proc Natl Acad Sci USA* 2005; **102**: 9182–9187.

34. Söllner TH. Intracellular and viral membrane fusion: a uniting mechanism. *Curr Opin Cell Biol* 2004; **16**: 429–435.

35. Chen MS, Tung KS, Coonrod SA, Takahashi Y, Bigler D, Chang A *et al.* Role of the integrin-associated protein CD9 in binding between sperm ADAM 2 and the egg integrin alpha6beta1: implications for murine fertilization. *Proc Natl Acad Sci USA* 1999; **96**: 11830–11835.

36. Lafuste P, Sonnet C, Chazaud B, Dreyfus PA, Gherardi RK, Wewer UM *et al.* ADAM12 and alpha9beta1 integrin are instrumental in human myogenic cell differentiation. *Mol Biol Cell* 2005; **16**: 861–870.

37. Albrechtsen R, Kveiborg M, Stautz D, Vikesâ J, Noer JB, Kotzsh A *et al.* ADAM12 redistributes and activates MMP-14, resulting in gelatin degradation, reduced apoptosis and increased tumor growth. *J Cell Sci* 2013; **126**: 4707–4720.

38. Fröhlich C, Kveiborg M, Stautz D, Vikesâ J, Noer JB, Kotzsh A *et al.* ADAM12 is expressed in the tumour vasculature and mediates ectodomain shedding of several membrane-anchored endothelial proteins. *Biochem J* 2013; **452**: 97–109.

39. Ito N, Nomura S, Iwase A, Ito T, Kikkawa F, Tsujimoto M *et al.* ADAMs, a disintegrin and metalloproteinases, mediate shedding of oxytocinase. *Bioch Biophys Res Comm* 2004; **314**: 1008–1013.

40. Brouxhon SM, Kyrkanides S, Teng X, Athar M, Ghazizadeh S, Simon M *et al.* Soluble E-cadherin: a critical oncogene modulating receptor tyrosine kinases, MAPK and PI3K/Akt/mTOR signaling. *Oncogene* 2014; **33**: 225–235.

41. Symowicz J, Adley BP, Gleason KJ, Johnson JJ, Ghosh S, Fishman DA *et al.* Engagement of collagen-binding integrins promotes matrix metalloproteinase-9-dependent E-cadherin ectodomain shedding in ovarian carcinoma cells. *Cancer Res* 2007; **67**: 2030–2039.

42. Fischer I, Weber M, Kuhn C, Fitzgerald JS, Schulze S, Friese K *et al.* Is galectin-1 a trigger for trophoblast cell fusion?: the MAP-kinase pathway and syncytium formation in trophoblast tumour cells BeWo. *Mol Hum Reprod* 2011; **17**: 747–757.

43. Nadeau V, Charron J. Essential role of the ERK/MAPK pathway in blood-placental barrier formation. *Development* 2014; **141**: 2825–2837.

44. Matsuura K, Jigami T, Taniue K, Morishita Y, Adachi S, Senda T *et al.* Identification of a link between Wnt/β-catenin signalling and the cell fusion pathway. *Nat Commun* 2011; **2**: 548.

45. Joshi PA, Jackson HW, Beristain AG, Di Grappa MA, Mote PA, Clarke CL *et al.* Progesterone induces adult mammary stem cell expansion. *Nature* 2010; **465**: 803–807.

46. Beristain AG, Molyneux SD, Joshi PA, Pomroy NC, Di Grappa MA, Chang MC *et al.* PKA signaling drives mammary tumorigenesis through Src. *Oncogene* 2014; **34**: 1160–1173.

47. Hogg K, Robinson WP, Beristain AG. Activation of endocrine-related gene expression in placental choriocarcinoma cell lines following DNA methylation knock-down. *Mol Hum Reprod* 2014; **20**: 677–689.

Supplementary Information accompanies this paper on Cell Death and Differentiation website (http://www.nature.com/cdd)